Review

Bridging structural and cell biology with cryo-electron microscopy

https://doi.org/10.1038/s41586-024-07198-2

Received: 18 July 2023

Accepted: 13 February 2024

Published online: 3 April 2024

Check for updates

Eva Nogales[1,2,3] ✉ & Julia Mahamid[4,5] ✉

Most life scientists would agree that understanding how cellular processes work requires structural knowledge about the macromolecules involved. For example, deciphering the double-helical nature of DNA revealed essential aspects of how genetic information is stored, copied and repaired. Yet, being reductionist in nature, structural biology requires the purification of large amounts of macromolecules, often trimmed off larger functional units. The advent of cryogenic electron microscopy (cryo-EM) greatly facilitated the study of large, functional complexes and generally of samples that are hard to express, purify and/or crystallize. Nevertheless, cryo-EM still requires purification and thus visualization outside of the natural context in which macromolecules operate and coexist. Conversely, cell biologists have been imaging cells using a number of fast-evolving techniques that keep expanding their spatial and temporal reach, but always far from the resolution at which chemistry can be understood. Thus, structural and cell biology provide complementary, yet unconnected visions of the inner workings of cells. Here we discuss how the interplay between cryo-EM and cryo-electron tomography, as a connecting bridge to visualize macromolecules in situ, holds great promise to create comprehensive structural depictions of macromolecules as they interact in complex mixtures or, ultimately, inside the cell itself.

Imagine you could magically shrink, as in the movie *A Fantastic Voyage*, into the realm of the nanometre world, and that you could see, with your own eyes, the intricate molecular jungle filling up our cells (physical laws be darned!). For those of us who have trust in the 'seeing is believing' paradigm when it comes to molecular mechanisms, this is probably not an unusual dream. For decades, structural biologists have used a poor man's approach to such dreams by painstakingly purifying their biological macromolecules of interest out of their cellular context and using the tools of the trade to generate atomic models, with luck, in several functional states, to infer the chemical and physical rules that govern their function. This reductionist approach has populated the Protein Data Bank (PDB)[1] at an ever-increasing rate and has allowed us to generate a physical framework that integrates biochemical and biophysical data, maps human mutations, predicts or helps to improve small-molecule binding for therapeutic purposes or, in the wake of a global pandemic, to map viral mutations that escape our antibodies or could weaken the effectiveness of our vaccines. Valuable as our visualization of macromolecular structure is out of the context of the cell, it is clear that the tunnel vision it provides is only a small part of a bigger, more complex story that ultimately has to include the molecular sociology[2] that necessarily governs cellular function, as cell biologists will be ready to tell you. The closest thing to our dream so far has been to contemplate the fabulous and aesthetically pleasing imagery of cellular landscapes that David Goodsell has created using the PDB, other available data, and an incredible taste for colour[3] (Fig. 1).

Shrinking fantasies and beautiful drawings aside, macromolecules can be 'seen' both inside and outside our cells, just not with our eyes, not with light and not without some compromise. This Review explores the use of electrons and the study of frozen-in-time molecules and cells by the sister methodologies of single-particle cryo-EM and cryo-electron tomography (cryo-ET) (Box 1). It is not meant to detail the principles behind such techniques, nor is a comprehensive summary of exciting new structures and cellular landscapes, for which we direct the readers to some excellent recent reviews[4–8]. Instead, this Review is an attempt to look into the present and the future of how different combinations of electron microscopy methods that visualize cryogenically preserved biological samples with different levels of complexity can bring us closer to our ultimate dream of understanding how macromolecules operate inside our cells to generate the adaptive and responsive complexity of the biological world.

Cryo-EM, a technique born several decades ago but that has gained centre stage among structural biology methods in the past decade[9], has several advantages with respect to X-ray crystallography or NMR, including the fact that, typically, much less sample material is needed and that there is no upper limit in the size of the macromolecule under study. These properties have made cryo-EM the method of choice to study many 'omes', that is, the (reasonably) stable complex molecular machinery that govern, among others, the central dogma (for example, DNA replication[10] and repair[11], transcription[12], splicing[13], translation[14], protein folding[15] and protein degradation[16], among others), to obtain

[1]Molecular and Cell Biology Department, Institute for Quantitative Biomedicine, University of California, Berkeley, CA, USA. [2]Molecular Biophysics and Integrated Bioimaging, Lawrence Berkeley National Laboratory, Berkeley, CA, USA. [3]Howard Hughes Medical Institute, Berkeley, CA, USA. [4]Structural and Computational Biology Unit, European Molecular Biology Laboratory (EMBL), Heidelberg, Germany. [5]Cell Biology and Biophysics Unit, European Molecular Biology Laboratory (EMBL), Heidelberg, Germany. ✉e-mail: enogales@lbl.gov; julia.mahamid@embl.de

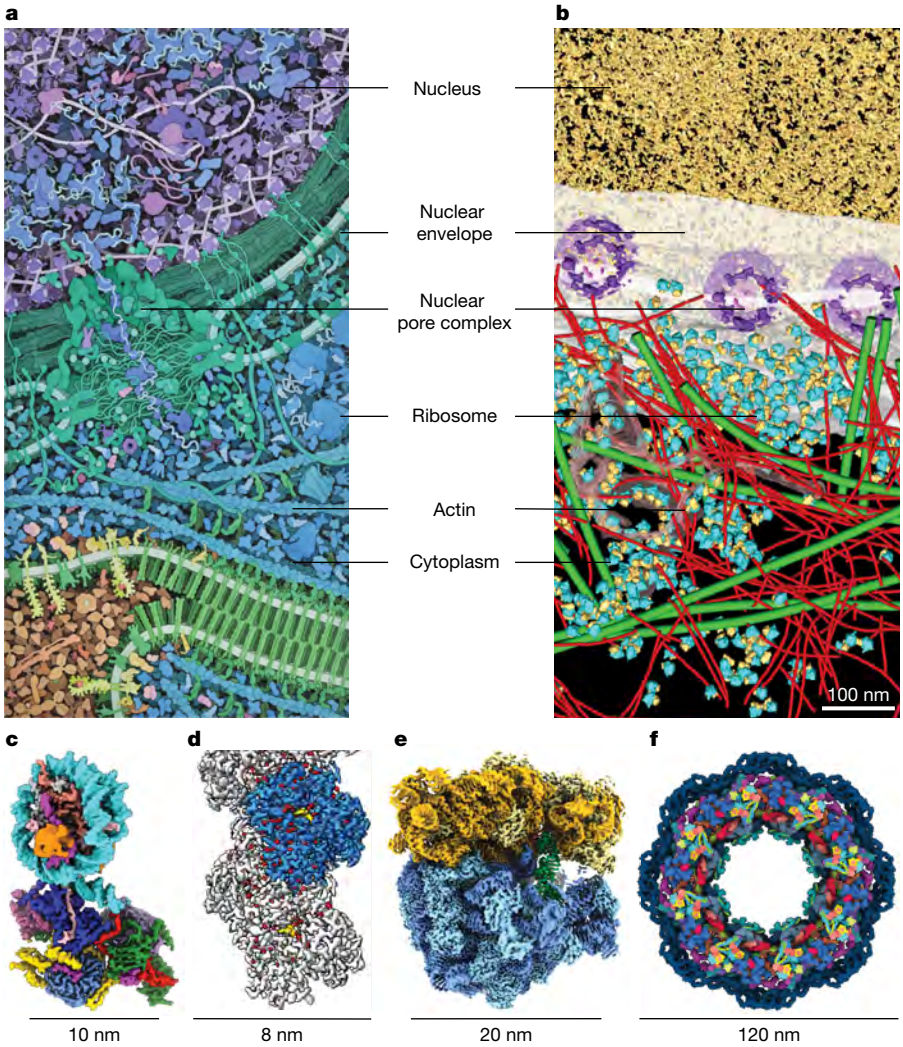

Fig. 1 | A structural biologist's dream. a, Illustration by D. Goodsell depicting the VEGF signalling pathway. Blood serum is at the bottom left. Cell membranes are shown in green, with the VEGF receptor in yellow-green and a disassembling adherent junction in darker green at the bottom. Multiple kinases (pink) are activated and travel through the cytoplasm (blue) and the nuclear pore (green; centre) to phosphorylate transcription factors in the nucleus (purple). Adapted with permission from ref. 3, copyright © 1999–2024 John Wiley & Sons, Inc. or related companies. **b**, Annotated rendering of cryo-ET data depicting a HeLa cell nuclear periphery. The nuclear envelope (transparent white) with nuclear pore complexes (purple) separates the nucleus (gold) from the cytoplasm containing ribosomes (blue and yellow), microtubules (green) and actin (red). Adapted with permission from ref. 118, AAAS. **c**–**e**, High-resolution reconstructions of macromolecular assemblies visualized in vitro by cryo-EM. **c**, Human Polycomb repressive complex 2 (PRC2) at approximately 3.5 Å resolution interacting with a nucleosomal substrate (DNA shown in cyan) recognizing a ubiquitin in histone H2A (orange) as the SET domain of EZH2 (blue) engages the histone H3 tail (pink) for methylation. Other domains of EZH2 are shown in yellow and maroon, EED in light blue, SUZ12 in green, RBAP48 in grey, AEBP2 in red and JARID2 in magenta. Adapted with permission from ref. 119, AAAS. **d**, Actin filaments in the Mg^{2+}–ADP–BeF_3^- state at approximately 2.2 Å resolution. One actin subunit is coloured blue, the nucleotide is yellow and ordered waters are red. Adapted from ref. 21, CC BY 4.0. **e**, Bacterial translating ribosome at 1.55 Å resolution coloured in dark yellow (16S rRNA), light yellow (ribosomal proteins in the small subunit), light blue (large subunit ribosomal proteins) and dark blue (23S and 5S rRNA). Adapted from ref. 14, CC BY 4.0. **f**, A structural model of the human nuclear pore complex built using integrative structural modelling with AlphaFold2 and a density map from cryo-ET of isolated nuclei. Adapted with permission from ref. 120, AAAS.

the structure of integral membrane proteins such as ion channels[17], viral proteins[18], signalling complexes[19] or photosynthesis complexes[20], or to visualize biological polymers at ever increasing resolution[21,22]. During the past decade, methodological improvements in cryo-EM have increased its throughput, applicability and resolution (now with demonstrated true atomic resolution for both simple test samples[23] and large complex assemblies[14]), greatly enhancing the biological insight that this method has been able to provide. In parallel, cryo-ET, which promises in situ visualization of all those macromolecules as they interact with each other in the complex cellular milieu, has started to overcome some of the technical hurdles inherent to the study of cells[4,24]: the need to generate thin samples (via mechanical cryo-sectioning[25–27] or now more often by focused ion beam (FIB) milling[28–31]), the compromised quality of images of tilted samples while maintaining a tolerable electron dose, the limited resolution in the subsequent tomographic reconstructions, or the interpretability of those cellular volumes permitted by the low signal-to-noise ratio compounded by the dense and complex nature of the cell[32]. If you are interested in a particular biological process, you are likely to consider the use of both methods. In fact, the two techniques can feed each other to provide biological insight that is more than the sum of their parts. For example, the high-resolution structures of large macromolecular complexes, polymers or membrane proteins, as obtained by cryo-EM of purified complexes, can help to find those structures in the cell when seen in

Box 1

Differences between cryo-EM and cryo-ET

Although in both cryo-EM and cryo-ET the samples are imaged in a frozen-hydrated vitreous state and using a transmission electron microscope of similar if not identical configuration, there are fundamental differences between the two methodologies (for some classical references on vitrification and 3D reconstruction principles, see refs. 26,124–127).

Most obviously, they differ in the data collection strategy used: single images (cryo-EM) versus tilt series (cryo-ET). When the object is imaged only once, the full electron dose allowed by radiation damage can be used to generate a high signal-to-noise ratio, and therefore a high-resolution image. Typically, thousands of images are taken, each one containing between tens and hundreds of 'particles', to generate datasets containing hundreds of thousands, if not millions, of particle images of the biological molecule of interest. A central assumption is that the particles are sufficiently self-consistent and that they are viewed in different orientations. Through a computational pipeline[128] that involves alignment and classification schemes, in both 2D and 3D, and a refinement that iteratively defines the relative angles of the different views being analysed, the selected images are merged together in one or several reconstructions that, if successful, result in density maps of sufficient resolution to allow the generation of an atomic model (typically at better than 4 Å resolution). However, in complex samples, such as inside the cell, particles densely stacked along the projection direction will produce overlapping signal in the 2D image. Typically, instead of taking a single image of a particular area in such samples, a series of images is acquired at different tilts, and the dose is fractionated across the multiple tilt images. Thus, each image in the tilt series has a low signal-to-noise ratio, which progressively deteriorates as the sample is tilted to higher angles owing to the thicker effective cross-section that the beam must go through. Using a pipeline that involves alignment of the tilt images in 2D, followed by 3D reconstruction, a tomographic volume is generated with improved signal-to-noise ratio and contrast over the individual images. This 3D volume, or tomogram, contains a somewhat distorted representation of the macromolecular 3D structures; although the original images are typically collected at 1–4 Å per pixel, tomograms show resolvable details only in the 2–5-nm range. This deteriorated resolution originates from technical limitations of tilting the stage inside the electron microscope and the restricting sample grid geometry, leading to incomplete sampling ('missing wedge'), and from the substantial non-linear deformation and damage that the biological material experiences when bombarded with the large number of electrons required to generate a tilt series (in the range of 120 e^{-} $Å^{-2}$). These limiting factors can be mitigated by the generation of subtomogram averages when self-consistent structures viewed in different orientations exist in the 3D tomograms, a process that involves alignment, classification and merging of the selected particles into reconstructions, similarly to how it is done in single-particle cryo-EM. This practice has started to yield resolutions better than 7 Å (refs. 41,42,121,129–133).

cryo-tomograms, or subtomogram averages of a certain complex as obtained from analysis of cryo-ET data can be interpreted by comparison with those structures of the complex obtained under controlled in vitro conditions. There are clearly multiple experimental paths across both techniques, and here we propose some that can be used in synergy to gain mechanistic information in the pursuit of a certain biological process. These combinations of experimental strategies are probably not the only ones possible.

Technical advances in cryo-EM and cryo-ET

Several technological breakthroughs have transformed the capabilities of both cryo-EM and cryo-ET over the past decade. Arguably, the most dramatic effect on both methods has come from the development and commercialization of better detector technology. The so-called direct electron detectors (DEDs) have greatly improved the contrast and resolution of the images[33]. Improving quantum efficiency and allowing for the correction of beam-induced motion (through alignment of video frames permitted by the fast readout of the cameras)[34] have both contributed to the highly improved performance of DEDs with respect to film. Automation of data collection and advances in the optical system of modern microscopes have also contributed to the quality and quantity of the images obtained and have led to both the general applicability of cryo-EM and its much-improved resolution. When it comes to cryo-ET of intact cells, where the major bottleneck for decades had been thinning of the sample to electron transparency, the adaptation of FIB milling, commonly used in the material sciences, to cryogenic samples finally provided an essential and routine solution that substantially minimizes perturbation to the sample[28–31,35–37] compared with traditional cryo-sectioning[25].

Perhaps as important as the hardware advances is the development of new software platforms that have taken advantage of the improved images and of Bayesian approaches to separate conformational or compositional states of the sample and discard contaminating or damaged particles that had contributed negatively to cryo-EM reconstructions[38–40]. Schemes of 2D and 3D classification are now nested within the pipeline of image analysis, in ways that are still often sample- and user-specific. These have allowed the improvement of resolution and often also describe, to different extents, the conformational landscape of the molecule under study. Although streamlined software solutions are now developed for the analysis of single-particle cryo-EM data, processing of cryo-ET data faces similar challenges and is handled through analogous, although more involved and somewhat less effective, pipelines[41–43]. Furthermore, visualizing functional molecules within the cellular context inherently involves capturing a potentially wide variety of interaction partners and/or conformations, which will require powerful software to untangle such complexity during the generation and analysis of subtomogram averages. New machine learning methodologies are also addressing the challenge of describing continuous conformational changes in macromolecules[40,44,45] and thus have the potential to provide novel insights into the complex conformational landscapes that are often at the heart of macromolecular function.

Sample complexity in cryo-EM and cryo-ET

The nature of the sample under study will be what ultimately determines which imaging technique to use (Fig. 2). In cryo-EM, the assumption is that the object being studied is simple in terms of compositional and conformational variation: for example, purified ribosomes (although probably in multiple states) would typically be the subject of cryo-EM. Conversely, higher-order assemblies of ribosomes in polysomes present in a cell will be imaged via cryo-ET. This reasoning takes us back to the initial consideration of cryo-EM as a more 'classical' reductionist, structural biology method, whereas cryo-ET holds the promise

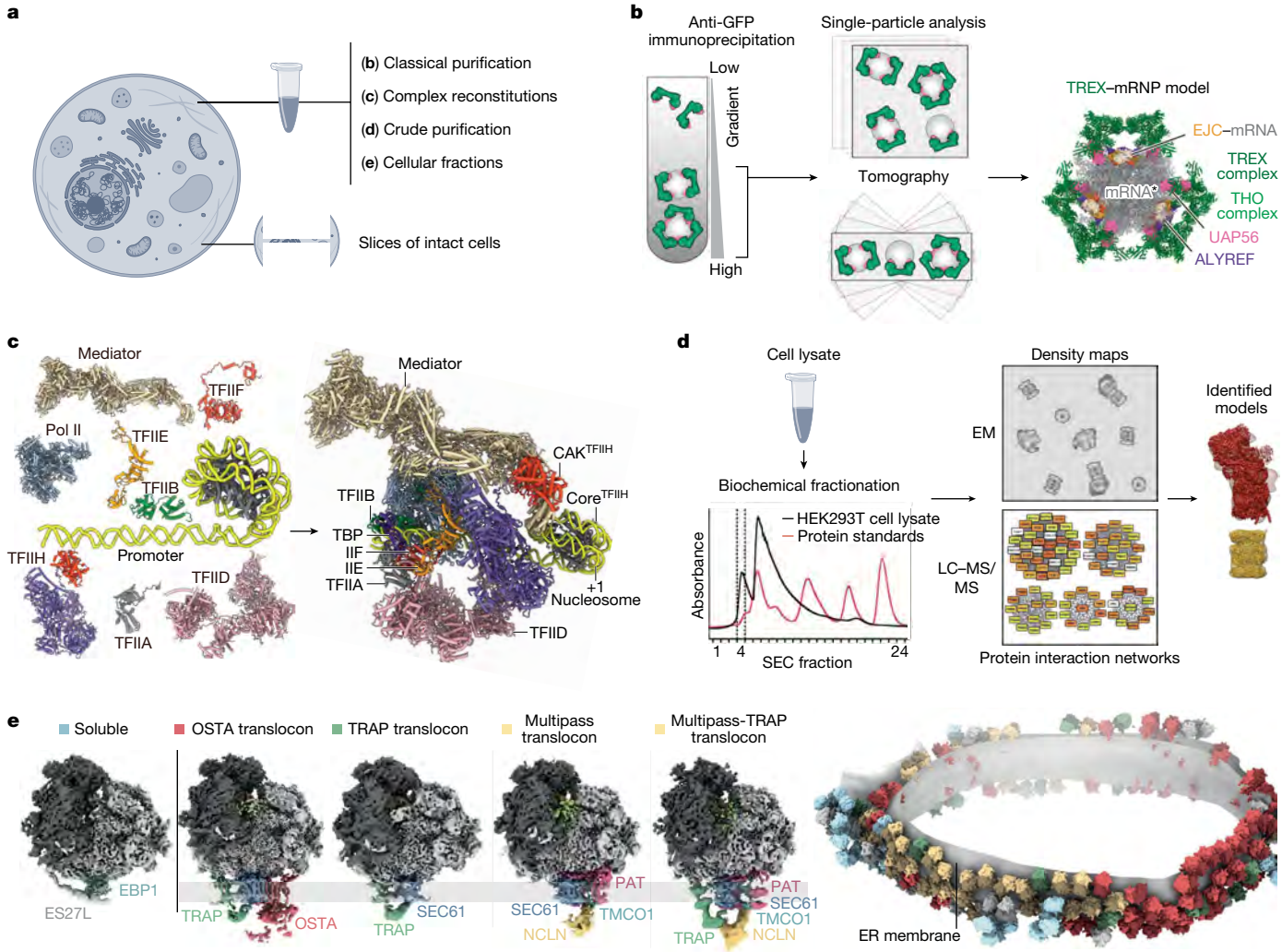

Fig. 2 | Characterizing Increasing sample complexity by a continuum of cryo-EM methods. a, Overview of the spectrum of samples for cryo-EM or cryo-ET. **b**, Pulldown on a GFP-tagged subunit of the TREX complex directly from a nuclear extract followed by sucrose gradient fractionation provided samples for both high-resolution single-particle cryo-EM and cryo-ET of ribonuclear particles (RNPs), leading to the determination of a pleomorphic mRNA core bounded by structurally defined TREX complexes necessary for nuclear export of RNPs. mRNA* indicates place holder mRNA derived from the human ribosome, as no structure of the pleomorphic mRNA in RNPs exists. Adapted from ref. 60, Springer Nature Ltd. **c**, In vitro reconstitution of the pre-initiation complex (PIC)–mediator supracomplex on chromatinized core promoter DNA from individual complexes (left) allowed cryo-EM analysis that led to a structural model for the full functional assembly (right). Adapted with permission from ref. 12, AAAS. **d**, Pipeline for structural analysis of heterogeneous mixtures of human cell lysates, combining shotgun cryo-EM analysis and classification with protein identification by mass spectrometry. LC–MS/MS, liquid chromatography–tandem mass spectrometry; SEC, size-exclusion chromatography. Adapted from ref. 63, CC BY 4.0. **e**, Complex ribosomal assemblies engaged with the integral-membrane translocon studied in situ by cryo-ET of microsomal fractions from human cells (right). The protein-conducting channel SEC61 associates with distinct combinations of cofactors, such as TRAP and OSTA (left), reflecting the requirements of different protein substrates in cells. Colours next to headings correspond with colours of individual particles shown in the rightmost image. Adapted from ref. 121, CC BY 4.0.

of imaging the cellular content in its somewhat chaotic and complex beauty. However, there is almost a continuum in the nature of the complexity of a sample; this spectrum necessarily challenges simple distinctions and blurs the boundaries of when one method or the other can be used. What follows is a proposal of different levels of sample complexity and the role that cryo-EM and cryo-ET can have in their structural characterization.

Traditional sample purification

The pipeline of sample preparation for cryo-EM often parallels that used for traditional structure determination, for example, by X-ray crystallography: overexpression of the macromolecule or complex in a heterologous system followed by strict purification aiming for a single biochemical species. However, because there is no need to obtain crystals, and because of the nature of electron scattering, typically much less sample is required for cryo-EM. Thus, biological samples that are traditionally hard to overexpress in large amounts, such as integral membrane proteins[46,47] (which can even be studied embedded in lipids[48]) or large complexes of many components[49–51], are more accessible by cryo-EM. But it is even more important to mention that the light requirements in terms of sample concentration for cryo-EM mean that it is possible to rely on endogenously purified material for structural studies, even when the complex pursued is present in low abundance in cells[52]. A general strategy could be to CRISPR-engineer a cell line in which one of the subunits of a complex of interest has been chromosomally tagged for affinity purification[53,54]. The advantage of this method is that the purification scheme can be relatively simple and preserve the integrity of assemblies, so as to guarantee a close resemblance to the state of the complex in the cell, including subunit composition and post-translational modifications. Samples can then

be concentrated for imaging via different forms of 'affinity grids'[55–57]. Although this 'milder' purification scheme may lead to samples of increased biochemical complexity (which could be defined via mass spectrometry), it is probably still constrained to a finite number of molecular entities that can be dealt with using single-particle cryo-EM principles. Furthermore, the arrival at a single species may not be easily achievable, and in some cases, not even desired. In cases where a limited number of macromolecules (for example, 2–5) co-purify in the chosen final step (for example, membrane fractions from an organelle that are separated in a sucrose gradient[58]), it has proven possible to deal with the different species simultaneously during cryo-EM data processing. The system still needs to be simple enough to have a defined parts list that would help with the processing by guiding the number of species expected during classification and reconstruction. Conversely, purified samples that are nevertheless pleomorphic, such as enveloped viruses[59] or ribonuclear particles that have an ill-defined stoichiometry[60], are typically considered more suitable for cryo-ET characterization.

Complex reconstitutions

When the system reconstituted from purified components gains in complexity owing to the number of molecular parts and/or unique arrangements of those parts (for example, multiple interactors bound to a cytoskeletal polymer[61] or coat protein–membrane assemblies[62]), it may be necessary to use non-trivial, tailored single-particle schemes to deal with this complexity, or cryo-ET followed by subtomogram averaging and classification. Collecting both modalities of data and analysing those datasets in parallel for systematic comparison of the resulting structures and interpretation may prove to be the most robust way to gain functional conclusions in some of the most complex reconstituted systems.

Crude purifications

It has become possible to relax the 'extraction' process to deal with only partially purified material (for example, size-exclusion fractions of a cell lysate) and pursue the simultaneous cryo-EM reconstruction of several macromolecules from a single grid or dataset of a highly complex mixture. In this way, a chromatographic method is used to separate components into 'bins' on the basis of size or charge, and different fractions are analysed in consecutive cryo-EM studies. Examples include human cell extracts[63], eukaryotic thermophile cell extracts[64], malaria parasite cell lysates[65] and detergent-solubilized membrane pellets from bacteria[66]. Such approaches are faced with the challenge of grouping the single-particle cryo-EM images according to different structures when there is no or little pre-existing knowledge of such structures, or even of how many should be expected to be present (here, mass spectrometry can provide some useful information). As of today, the process cannot be done reliably without some human intervention in the early stages of generating initial models, and so far, its implementation has concentrated on the most abundant and/or featureful (large, symmetric) molecules. In this context, a more objective way of generating initial models to seed the image analysis process, with the potential to pursue the structure determination in a more systematic way, should be considered. One possibility would be to obtain cryo-ET data from the same sample grid to generate initial models. Whether the 'raw' volumes would be sufficient or some subtomogram classification, not without its own limitations when dealing with highly heterogenous samples, needs to be carried out may depend on the nature of the molecules and the quality of the tomograms. Imaging schemes that maximize the signal, such as phase plates[67,68], may be beneficial to simplify the process of generating initial models from cryo-ET that can be used for cryo-EM analysis of complex mixtures.

Cell fractions

A bootstrapping step moving from purified systems, of any complexity, to looking inside a cell is the visualization of cellular fractions. Extracts and cell fractions have been broadly used for decades to elucidate cellular pathways. In the context of cryo-EM imaging in the transmission electron microscope, the advantages of the extract over working with intact cells include overcoming the bottleneck of generating thin cellular sections, and the opportunity to manipulate the extract to either remove components (for example, by immunodepletion) or by adding them, via overexpression in cell culture systems or by exogenous addition[69]. In the latter case, added key components could be fluorescently labelled so that they can be followed by correlative light and electron microscopy (CLEM) methods, or even labelled with an electron-dense marker for direct identification in cryo-EM, without the need of generating a more complex in vivo labelling scheme. The benefit of the extract with respect to a complex reconstitution is that it does not involve purification of components, which in some cases faces technical bottlenecks. It also provides a more physiological environment where functionally relevant partners that may not yet be known are present and where the 'crowdedness' of the cellular milieu can be maintained if desired. More recently, methods have emerged that combine microfluidic single-cell extraction with single-particle analysis by electron microscopy to characterize protein complexes from individual *Caenorhabditis elegans* embryos[70]. Conversely, working with cell extracts is a compromise in which interpretation may be just as difficult as in an in situ study, yet in which the true cellular context has been lost. In general, it is likely that these systems will need to be studied by cryo-ET.

Working with intact cells

In many cases, the biological question being addressed will require looking directly into the cell or tissue. If a molecular interpretation of the cellular landscape is desired, the cell or tissue will first have to be vitrified. Depending on the original thickness of the biological object, traditional plunge freezing can be used (for example, for single cells)[26] or high-pressure freezing[71] may be required (for multicellular or tissue samples). Regardless of the vitrification method, the ideal sample for analysis with a reasonable signal-to-noise ratio requires a sample thickness of less than 0.3 µm (and ideally half of that). This can be accomplished via cryo-sectioning or, more commonly these days, via FIB milling[28,29], typically coupled to scanning electron microscopy (SEM) to monitor the process and visualize the resulting lamella. These thin sections or lamellae will be the ones introduced into the transmission electron microscope and imaged, most commonly, via cryo-ET. Until recently, cellular thinning and high-quality cryo-ET data acquisition on FIB lamellae were accessible to just a few experts. However, the increasing availability of commercial, out-of-the-box hardware solutions[72], knowledge transfer and standardization of sample preparation[31,73,74], innovation in integrated instrumentation (for example, inclusion of a light microscope in the FIB chamber[75–78] to minimize cumbersome sample transfers between microscopes), and automation in both FIB preparations[79,80] and large-scale cryo-ET imaging[81–83] are gradually making these methods more widely available across the life sciences and to non-expert communities through service provisions in large facilities and centres.

Extracting information in complex samples

What kind of information can be obtained when the complexity or nature of the sample requires cryo-ET? Cryo-tomograms are often interpreted after some denoising[84–86], segmentation and/or localization of the most obvious elements, such as membranes, cytoskeletal polymers and large macromolecular assemblies such as ribosomes. The identification of the structures of interest in the cellular milieu (or in complex mixtures/cellular extracts) can be performed by computational pattern recognition using, for example, templates from high-resolution structures and matching them with the tomograms (as discussed below) employing either traditional cross-correlation[87], supervised deep-learning[88,89] or by unsupervised algorithms[90] (which

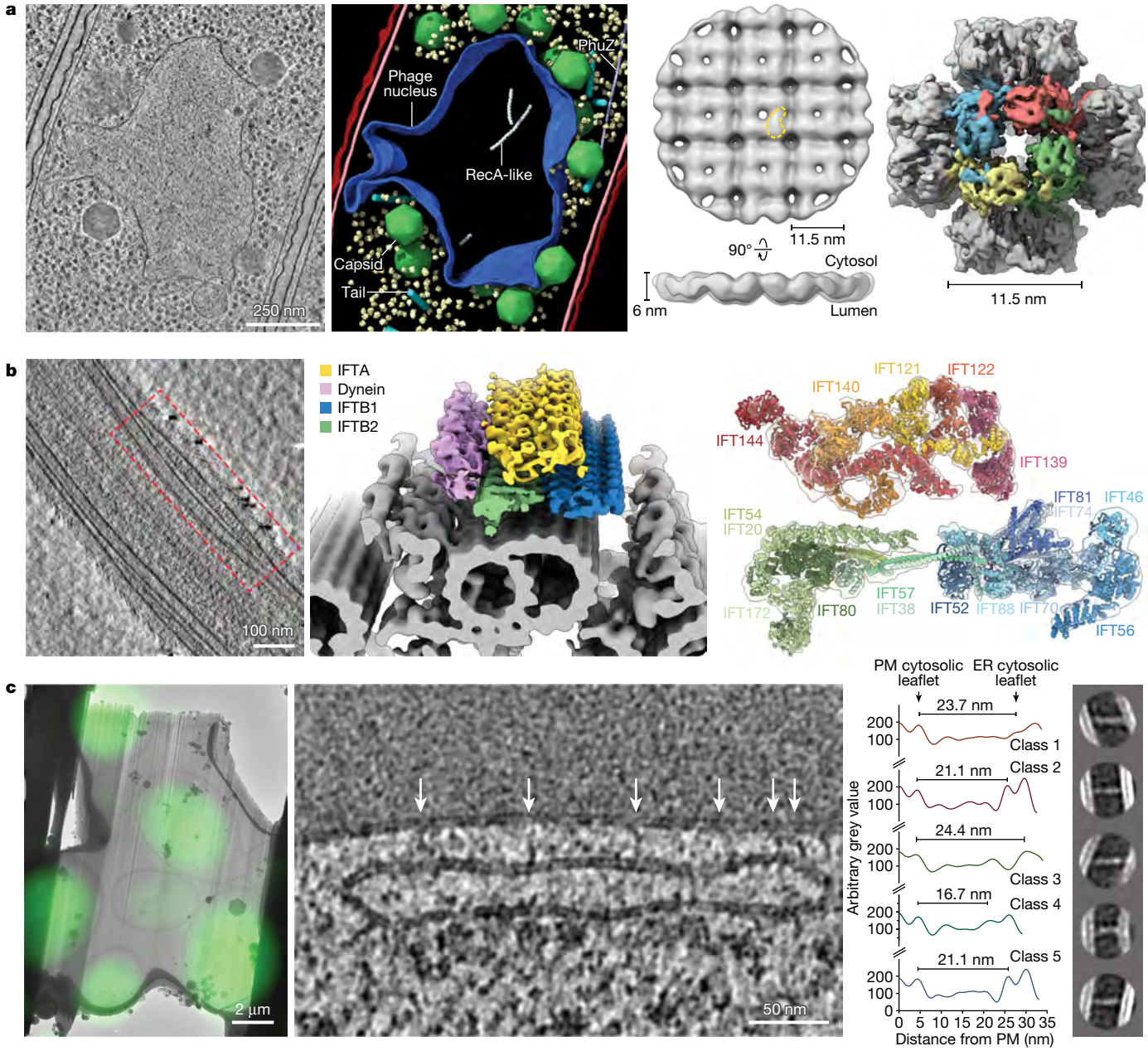

Fig. 3 | Cryo-ET visualizes complex cell biology. a, Cryo-ET study of bacteriophage-infected bacterial cells and reconstituted bacteriophage assemblies. The phage assembles a nuclear shell from one protein (chimallin A). From left to right: tomographic slice; segmented cryo-tomogram; subtomogram average of the phage 'nucleus' and structure resolved by cryo-ET of a minimal chimallin shell reconstituted in vitro. Adapted from ref. 104, CC BY 4.0. **b**, Cryo-ET of intact *Chlamydomonas reinhardtii* cilia combined with cross-linking-mass spectrometry and AlphaFold predictions reveals the intraflagellar transport machinery or trains (IFT). From left to right: tomographic slice; a composite map obtained from subtomograms averaging of four IFT components showing the independently refined domains of the anterograde trains positioned above the microtubule doublet (grey), with IFTB1 (blue), IFTB2 (green), dynein (pink) and IFTA (yellow); and a structural model of IFTA and IFTB derived from AlphaFold2 and fitted into the cryo-ET density using molecular dynamics flexible fitting. Adapted from ref. 105, CC BY 4.0. **c**, Cryo-CLEM of a FIB lamella with quantitative measurements and sub-tomogram classification to study organelle contacts between the endoplasmic reticulum (ER) and plasma membrane (PM) in budding yeast. From left to right: overlay of cryo-fluorescence microscopy image (GFP channel, acquired before FIB milling) and cryo-EM image of a lamellae of cells expressing GCaMP, a fluorescent indicator of intracellular Ca^{2+} concentration; a tomographic slice showing ER–PM contacts (arrows) in a cell overexpressing Tcb3–eGFP; and density projection profiles along the major axis of the bridges seen in the 2D class averages (right most) obtained by subtomogram averaging of the bridge structures. For each profile, the indicated length measured between the cytosolic leaflets of the PM and the ER provides an estimate of the length of the different bridge classes. Adapted from ref. 122, CC BY 4.0.

still require substantial developments and validation). There are two additional alternative approaches for particle identification based on tagging the component of interest. The first involves the use of correlated light and electron microscopy of fluorescently tagged complexes[91–94], for which methodologies are being developed to overcome the diffraction limit of light (that is, super-resolution approaches) to achieve registration precision on the scale of 10 nm in cryogenically preserved samples[95–97]. The second entails the use of molecular tags that can directly pinpoint the location of the complex of interest in cryo-tomograms. Current applications involve either electron-dense particles that produce high contrast in the electron microscope[98] or self-assembling particles with distinct shapes

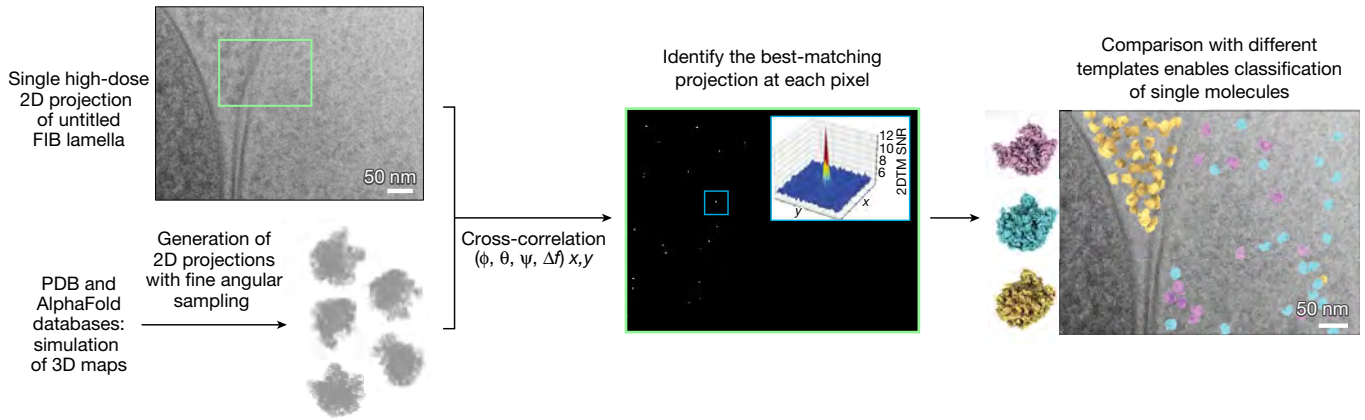

Fig. 4 | In situ cryo-EM with 2D template matching. Pipeline for the use of 2D template matching: high-dose, high-resolution 2D projection images of a cellular slice (from FIB milling, top left) are matched against (a number of) available high-resolution structures from structural databases or structure prediction (bottom left); high correlation scores indicate the presence of the template in the cellular volume (centre), allowing the identified structures to be positioned in the cellular context (right). Adapted from ref. 123, CC BY 4.0.

that can be identified using template matching or machine learning algorithms[99,100].

Bona fide structural understanding will often require analyses that go beyond segmentation and localization. Similar to single-particle ryo-EM, obtaining a molecular structure from cryo-ET requires averaging and classifying multiple copies of similar entities, especially when attempting to disentangle variability with a higher level of detail and resolution. Therefore, populations of conformations with low abundance can be easily missed. Although in single-particle cryo-EM this is typically addressed by enriching the particular entity or state in the specimen, acquiring large numbers of particle images, and using classification schemes, for cryo-ET of intact cells, a brute force approach for higher-throughput data collection is typically the only way to achieve this. Cryo-ET is limited in throughput compared with cryo-EM, although recent developments[82,101] have dramatically improved the speed at which tomograms can be collected. It is also important to note that despite the power of FIB–SEM to produce thin cellular lamellae, this methodology is still not perfect, and samples are not entirely undamaged by the thinning process[102,103]. Contrast also remains a limitation in cryo-ET. Thicker and more-complex samples result in necessarily reduced contrast compared with that obtained from purified cryo-EM samples. Finally, non-trivial sample preparation and analysis pipelines still require substantial expertise and painstakingly acquired knowledge of experimental details. Nevertheless, combinations of the technical advances mentioned above will soon lead to the generation of thousands of tomograms for each biological process or object of interest. As they stand, current applications of state-of-the-art cryo-ET, in its different flavours and in combination with correlative methods, are already providing unprecedented insights into complex cell biology, even when they do not produce high-resolution subtomogram averages from macromolecules imaged in situ. A few breath-taking examples include bacterial cell biology of phage infection[104], the exceptionally complex regulation of molecular transport in specialized cellular subcompartments[105] and of interorganelle membrane contact sites in eukaryotes[106] (Fig. 3). These examples represent only a glimpse into the outstanding impact cryo-ET, when integrated with structural modelling, will likely have in bridging structural and cell biology.

Interplay between cryo-EM and cryo-ET

Because the resolution of structures that can be generated by cryo-ET is often lower than that of cryo-EM, but the former provides a more physiological context all the way to the native cell or tissue, the two approaches are naturally complimentary. As noted above, cryo-EM is inherently reductionist in nature, although it can readily deal with large assemblies containing many subunits and therefore study fully biochemically functional complexes. The more transient interactions of such 'stable' complexes with regulatory factors can also be studied in this way. These supramolecular assemblies are very likely to resemble those in mild purifications, extracts or inside the cell. Thus, cryo-EM structures are ideal to interpret lower-resolution cryo-ET maps derived from more complex systems (for example, extracts and cells). Additional complementary structural methods, both experimental and computational (that is, predictions[107,108]) can also be used. Although integrative modelling can be used to combine predicted structures of individual components with additional information, such as crosslinking mass spectrometry[109,110], large complexes are not yet in the realm of what can be systematically predicted. Therefore, the larger molecular sizes studied by cryo-EM, often providing multiple functional states, give it an advantage, and structures generated by cryo-EM can be readily used to interpret the complex cryo-ET reconstructions.

One obvious way in which cryo-EM and cryo-ET can be combined is to use cryo-EM structures as templates[87] to search tomographic volumes and identify the position of the corresponding molecule in the cellular context. The low signal in tomograms has so far restricted this approach to relatively large complexes, such as ribosomes or proteosomes, and this method has yet to be broadly successfully applied even to particles in the hundreds of kilodalton range. An alternative to 3D template matching on tomographic volumes is to perform 2D template matching in single, high-resolution images of cellular slices[111,112] (Fig. 4). Here the identification of the molecule of interest relies on high-resolution features in the image, and the accuracy in finding a match requires high similarity between the template and the biological object in the micrograph. Although the shortcoming is that the precise high-resolution structure may not be available, the upside is that the method should be able to discriminate even different conformational states of each instance of the object (without resorting to averaging and classification) if such structures are available in the PDB or can be computationally generated (for instance, through molecular dynamics simulations). On the one hand, additional cofactors that interact with the complex in the native cellular context may be potentially recovered using alignment and averaging strategies analogous to single-particle cryo-EM[113]. Although algorithms are still being developed to carefully address the expected strong template bias, the mere emergence of such extra densities in the analysis (when they did not exist in the template) provides strong evidence that new structures could be obtained using 2D template matching and promise

Box 2

Cryo-EM and cryo-ET data accessibility

Many years ago, the maturity of the X-ray crystallography field both allowed and demanded that the coordinates of structural models be deposited following publication, so that the entire scientific community could mine the richness of information contained in such structures. The PDB[134] was born to host X-ray, NMR and the rare electron crystallography structure. As the single-particle cryo-EM field gained output and maturity, the same became a requirement for its structures and maps (the latter deposited in the Electron Microscopy Data Bank (EMDB)[135]). Image analysis developers have benefited from the availability of raw data which, in the case of electron microscopy, is deposited in the EMPIAR (Electron Microscopy Public Image Archive)[136]. The discussion on how to make available tomographic data is still open. It is clear that it would help to speed up technical developments and to increase the biological insight mined from each tomogram, thereby propelling the advancement of cryo-ET as an emerging method in structural biology. However, it is also clear that the community needs careful thought about cryo-ET data deposition that maintains meaningful connectivity across the substantially different data types, from the raw micrographs in a large number of tilt series, through reconstructed 3D volumes, coordinates of localized particles, annotations of their identified functional states and their mapping into the original cellular volumes in the form of 3D segmentations. It is important to also consider that the latter data types would be of interest to researchers in different disciplines, such as cell biologists, who may not be familiar with file formats specific to the cryo-EM field. Therefore, for these data to be helpful, especially to those without a structural biology background, it is important to implement user-friendly visualization of the tomograms and segmentations, and to facilitate retrieval of quantified and localized particle data, which can describe, for example, the molecular concentrations of functional complexes and their distributions across different subcellular areas or cell states.

an exciting opportunity to complement cryo-ET approaches in obtaining high-resolution structures in situ. On the other hand, 2D template matching, by concentrating on specific molecular targets, does not provide a more complete view of their intracellular context (for example, a volumetric description of membranes, the cytoskeleton or other unknown molecular assemblies).

To date, both 3D and 2D template matching have been demonstrated only for a handful of large complexes and remain computationally expensive. How far each of these methods can go in identifying smaller complexes based on experimentally or computationally generated structures remains to be seen. Each method is likely to improve, both with better images obtained with new phase plate-based instruments and/or better detectors, and with the improvement of processing algorithms. Although the choice of one versus the other may depend on the biological question being asked, one option would be to obtain both cryo-EM and cryo-ET and carry out both 2D and 3D template matching on the same sample region. Both types of template matching could be done in parallel and the results compared[111]. When used sequentially, a lower-resolution tomogram (in this case, somewhat reduced in quality by the approximately 20 $e^{-} A^{-2}$ invested in a first 2D high-resolution projection) would visualize the 3D environment that gives context to the analysis by 2D template matching. Optimization of both approaches with the right type of test cases would allow objective validation, perhaps using more simplified systems, before we are able to move fully into the systematic analysis of complex cellular sociology that is ultimately the target.

Beyond cryo-EM and cryo-ET

The major advantage of studying intact cells by cryo-ET is its potential to capture the full set of macromolecules and their interaction partners in a context-dependent manner. However, the use of thin cellular slices (approximately 200 nm thickness) and the restricted field of view in the tomograms that is associated with the angstrom-range pixel sizes of the data, both required to achieve high-resolution imaging, greatly limit the region being visualized out of the full cell or multicellular specimen. Cryo-ET studies are often complemented by correlative imaging methods, most commonly fluorescence microscopy, sometimes with super-resolution methods, to provide essential knowledge on the location and identity of a subcellular structure or molecular assembly, both to guide the FIB milling process and the subsequent cryo-ET data collection and interpretation. However, fluorescence-based imaging suffers from the limitation of visualizing a selected number of tagged molecules or organelles. Owing to their non-selective contrast mechanisms, room temperature FIB–SEM[114,115] and SEM block face[116] volume imaging, and cryogenic X-ray tomography[117], are increasingly used to generate 3D data on cellular ultrastructure at resolutions spanning 10–50 nm. These methods reveal the intricate connectivity between cellular organelles, their abundance and distributions across entire cells, even within complex multicellular tissues or entire organisms. Ultimately, to connect molecular-level structures obtained by cryo-EM or cryo-ET to function at the cellular and organismal level will require further developments in large-volume imaging methods of frozen hydrated samples, which could then be followed by FIB milling and/or extraction of specific sections[35,37] for subsequent cryo-ET. Such methodology is starting to emerge and will mature over the coming years. Finally, with cryo-ET methods fast evolving on multiple fronts towards higher throughput, they could be complemented by the integration of multi-omics single-cell data (for example, high-throughput and quantitative light microscopy, transcriptomics, metabolomics and proteomics) to reveal the beautiful variability and stochasticity of biological processes across cells. When combined with high-resolution structures from cryo-EM of purified macromolecular complexes, a new mechanistic understanding of cellular processes and their regulation is sure to emerge.

The structural databases (see Box 2 for a perspective on past and future structure databases) have contributed to the emergence of transformative protein structure prediction, which has taken structural biology by storm. Although the world of structure prediction had progressed at a steady but frustrating pace for years, what artificial intelligence methods such as AlphaFold[108] or RosettaFold[107] can now do has elevated structure prediction to a totally new level. As the reach of these methods expands to predict complexes that include multiple protein chains, many even wonder what the future of experimental structural biology is. Obviously, artificial intelligence protein structure prediction can be a strong ally that augments the reach and speed of structural biology. Predictions may guide selection of samples to study or generate expectations concerning well versus poorly structured regions. Most importantly in an electron microscopy study, once a cryo-EM or cryo-ET density is available, predictions can speed up atomic model building by providing initial structures of all potential or actual parts of the complex, which can then be refined more carefully into the experimental density map. For in situ studies, predictions can be used to generate templates for 2D and 3D template matching, a principle that will become more applicable as the tomograms quality and template matching schemes allow detection of smaller entities and/or when predictions can be applied to large complexes with many subunits. What is clear is that today bootstrapped paths

from artificial intelligence-based predictions to cryo-EM experimental structures of large assemblies and to the interpretation of intracellular landscapes captured by cryo-ET in terms of molecular structure are already a reality.

1. Berman, H., Henrick, K. & Nakamura, H. Announcing the worldwide Protein Data Bank. *Nat. Struct. Biol.* **10**, 980 (2003).
2. Robinson, C. V., Sali, A. & Baumeister, W. The molecular sociology of the cell. *Nature* **450**, 973–982 (2007).
   This seminal review coined the term 'molecular sociology' and set the scene for future in situ structural biology that combines cryo-ET with proteomics via integrative modelling.
3. Span, E. A. et al. Protein structure in context: the molecular landscape of angiogenesis. *Biochem. Mol. Biol. Educ.* **41**, 213–223 (2013).
4. Bäuerlein, F. J. B. & Baumeister, W. Towards visual proteomics at high resolution. *J. Mol. Biol.* **433**, 167187 (2021).
5. Berger, C. et al. Cryo-electron tomography on focused ion beam lamellae transforms structural cell biology. *Nat. Methods* **20**, 499–511 (2023).
6. Chua, E. Y. D. et al. Better, faster, cheaper: recent advances in cryo-electron microscopy. *Annu. Rev. Biochem.* **91**, 1–32 (2022).
7. Wu, M. & Lander, G. C. Present and emerging methodologies in cryo-EM single-particle analysis. *Biophys. J.* **119**, 1281–1289 (2020).
8. Young, L. N. & Villa, E. Bringing structure to cell biology with cryo-electron tomography. *Annu. Rev. Biophys.* **52**, 573–595 (2023).
9. Kühlbrandt, W. The resolution revolution. *Science* **343**, 1443–1444 (2014).
10. Lewis, J. S. et al. Mechanism of replication origin melting nucleated by CMG helicase assembly. *Nature* **606**, 1007–1014 (2022).
11. Chen, S. et al. Structural basis of long-range to short-range synaptic transition in NHEJ. *Nature* **593**, 294–298 (2021).
12. Chen, X. et al. Structures of +1 nucleosome-bound PIC–Mediator complex. *Science* **378**, 62–68 (2022).
    This study is an inspiring example of the large size and complexity of reconstitution systems amenable for cryo-EM study. It visualized an assembly of eight transcription complexes, some over 1 MDa in size, on chromatin.
13. Tholen, J., Razew, M., Weis, F. & Galej, W. P. Structural basis of branch site recognition by the human spliceosome. *Science* **375**, 50–57 (2022).
14. Fromm, S. A. et al. The translating bacterial ribosome at 1.55 Å resolution generated by cryo-EM imaging services. *Nat. Commun.* **14**, 1095 (2023).
15. Gestaut, D. et al. Structural visualization of the tubulin folding pathway directed by human chaperonin TRiC/CCT. *Cell* **185**, 4770–4787.e20 (2022).
16. Bashore, C. et al. Targeted degradation via direct 26S proteasome recruitment. *Nat. Chem. Biol.* **19**, 55–63 (2023).
17. Zhang, K., Julius, D. & Cheng, Y. Structural snapshots of TRPV1 reveal mechanism of polymodal functionality. *Cell* **184**, 5138–5150.e12 (2021).
18. Kern, D. M. et al. Cryo-EM structure of SARS-CoV-2 ORF3a in lipid nanodiscs. *Nat. Struct. Mol. Biol.* **28**, 573–582 (2021).
19. Lin, X. et al. Cryo-EM structures of orphan GPR21 signaling complexes. *Nat. Commun.* **14**, 216 (2023).
20. Domínguez-Martín, M. A. et al. Structures of a phycobilisome in light-harvesting and photoprotected states. *Nature* **609**, 835–845 (2022).
21. Oosterheert, W., Klink, B. U., Belyy, A., Pospich, S. & Raunser, S. Structural basis of actin filament assembly and aging. *Nature* **611**, 374–379 (2022).
22. Reynolds, M. J., Hachicho, C., Carl, A. G., Gong, R. & Alushin, G. M. Bending forces and nucleotide state jointly regulate F-actin structure. *Nature* **611**, 380–386 (2022).
23. Nakane, T. et al. Single-particle cryo-EM at atomic resolution. *Nature* **587**, 152–156 (2020).
24. Beck, M. & Baumeister, W. Cryo-electron tomography: can it reveal the molecular sociology of cells in atomic detail? *Trends Cell Biol.* **26**, 825–837 (2016).
    A landmark review that discusses how recent technological breakthroughs in sample thinning, combined with direct electron detection and phase plates, hold promise to achieve near-atomic reconstructions by in situ cryo-ET.
25. Al-Amoudi, A., Studer, D. & Dubochet, J. Cutting artefacts and cutting process in vitreous sections for cryo-electron microscopy. *J. Struct. Biol.* **150**, 109–121 (2005).
26. McDowall, A. W. et al. Electron microscopy of frozen hydrated sections of vitreous ice and vitrified biological samples. *J. Microsc.* **131**, 1–9 (1983).
27. Gan, L., Ng, C. T., Chen, C. & Cai, S. A collection of yeast cellular electron cryotomography data. *Gigascience* **8**, giz077 (2019).
28. Marko, M., Hsieh, C., Schalek, R., Frank, J. & Mannella, C. Focused-ion-beam thinning of frozen-hydrated biological specimens for cryo-electron microscopy. *Nat. Methods* **4**, 215–217 (2007).
29. Rigort, A. et al. Focused ion beam micromachining of eukaryotic cells for cryoelectron tomography. *Proc. Natl Acad. Sci. USA* **109**, 4449–4454 (2012).
30. Schaffer, M. et al. Optimized cryo-focused ion beam sample preparation aimed at in situ structural studies of membrane proteins. *J. Struct. Biol.* **197**, 73–82 (2017).
31. Wagner, F. R. et al. Preparing samples from whole cells using focused-ion-beam milling for cryo-electron tomography. *Nat. Protoc.* **15**, 2041–2070 (2020).
32. Lucic, V., Rigort, A. & Baumeister, W. Cryo-electron tomography: the challenge of doing structural biology in situ. *J. Cell Biol.* **202**, 407–419 (2013).
33. Faruqi, A. R. & McMullan, G. Direct imaging detectors for electron microscopy. *Nucl. Instrum. Methods Phys. Res. Sect. A* **878**, 180–190 (2018).
34. Campbell, M. G. et al. Movies of ice-embedded particles enhance resolution in electron cryo-microscopy. *Structure* **20**, 1823–1828 (2012).
35. Schaffer, M. et al. A cryo-FIB lift-out technique enables molecular-resolution cryo-ET within native *Caenorhabditis elegans* tissue. *Nat. Methods* **16**, 757–762 (2019).
36. Kelley, K. et al. Waffle method: a general and flexible approach for improving throughput in FIB-milling. *Nat. Commun.* **13**, 1857 (2022).
37. Schiøtz, O. H. et al. Serial lift-out: sampling the molecular anatomy of whole organisms. *Nat. Methods* https://doi.org/10.1038/s41592-023-02113-5 (2023).
    This work presents developments that substantially improve success rates and reproducibility in cryo-FIB micromachining and micromanipulator-assisted lift-out for production of samples suitable for cryo-ET from small multicellular model organisms.
38. Punjani, A., Rubinstein, J. L., Fleet, D. J. & Brubaker, M. A. cryoSPARC: algorithms for rapid unsupervised cryo-EM structure determination. *Nat. Methods* **14**, 290–296 (2017).
39. Scheres, S. H. W. Processing of structurally heterogeneous cryo-EM data in RELION. *Methods Enzymol.* **579**, 125–157 (2016).
40. Zhong, E. D., Bepler, T., Berger, B. & Davis, J. H. CryoDRGN: reconstruction of heterogeneous cryo-EM structures using neural networks. *Nat. Methods* **18**, 176–185 (2021).
41. Tegunov, D., Xue, L., Dienemann, C., Cramer, P. & Mahamid, J. Multi-particle cryo-EM refinement with M visualizes ribosome-antibiotic complex at 3.5 Å in cells. *Nat. Methods* **18**, 186–193 (2021).
    This work developed algorithms that allowed correction of sample deformation during cryo-ET acquisition to obtain, to our knowledge, the first near-atomic reconstruction of a macromolecular complex inside cells.
42. Wan, W., Khavnekar, S., Wagner, J., Erdmann, P. & Baumeister, W. STOPGAP: a software package for subtomogram averaging and refinement. *Microsc. Microanal.* **26**, 2516 (2020).
43. Zivanov, J. et al. A Bayesian approach to single-particle electron cryo-tomography in RELION-4.0. *eLife* **11**, e83724 (2022).
44. Powell, B. M. & Davis, J. H. Learning structural heterogeneity from cryo-electron sub-tomograms with tomoDRGN. Preprint at *bioRxiv* https://doi.org/10.1101/2023.05.31.542975 (2023).
45. Rangan, R. et al. Deep reconstructing generative networks for visualizing dynamic biomolecules inside cells. Preprint at *bioRxiv* https://doi.org/10.1101/2023.08.18.553799 (2023).
46. Allard, C. A. H. et al. Structural basis of sensory receptor evolution in octopus. *Nature* **616**, 373–377 (2023).
47. Xu, W. et al. Structural basis for strychnine activation of human bitter taste receptor TAS2R46. *Science* **377**, 1298–1304 (2022).
48. Yao, X., Fan, X. & Yan, N. Cryo-EM analysis of a membrane protein embedded in the liposome. *Proc. Natl Acad. Sci. USA* **117**, 18497–18503 (2020).
49. Mühleip, A. et al. Structural basis of mitochondrial membrane bending by the I–II–III2–IV2 supercomplex. *Nature* **615**, 934–938 (2023).
50. Vallese, F. et al. Architecture of the human erythrocyte ankyrin-1 complex. *Nat. Struct. Mol. Biol.* **29**, 706–718 (2022).
51. Walton, T. et al. Axonemal structures reveal mechanoregulatory and disease mechanisms. *Nature* https://doi.org/10.1038/s41586-023-06140-2 (2023).
52. Abdella, R. et al. Structure of the human Mediator-bound transcription preinitiation complex. *Science* **372**, 52–56 (2021).
53. Herbst, D. A. et al. Structure of the human SAGA coactivator complex. *Nat. Struct. Mol. Biol.* **28**, 989–996 (2021).
54. Liu, H., Li, A., Rochaix, J.-D. & Liu, Z. Architecture of chloroplast TOC–TIC translocon supercomplex. *Nature* **615**, 349–357 (2023).
55. Kelly, D. F., Abeyrathne, P. D., Dukovski, D. & Walz, T. The affinity grid: a pre-fabricated EM grid for monolayer purification. *J. Mol. Biol.* **382**, 423–433 (2008).
56. Han, B.-G. et al. Long shelf-life streptavidin support-films suitable for electron microscopy of biological macromolecules. *J. Struct. Biol.* **195**, 238–244 (2016).
57. Wang, F. et al. General and robust covalently linked graphene oxide affinity grids for high-resolution cryo-EM. *Proc. Natl Acad. Sci. USA* **117**, 24269–24273 (2020).
58. Maldonado, M., Guo, F. & Letts, J. A. Atomic structures of respiratory complex III2, complex IV, and supercomplex III2–IV from vascular plants. *eLife* **10**, e62047 (2021).
59. Peukes, J. et al. The native structure of the assembled matrix protein 1 of influenza A virus. *Nature* **587**, 495–498 (2020).
60. Pacheco-Fiallos, B. et al. mRNA recognition and packaging by the human transcription–export complex. *Nature* **616**, 828–835 (2023).
    This study is an example of the combination of single-particle cryo-EM and cryo-ET in the structural characterization of a complex biological assembly.
61. Ferro, L. S. et al. Structural and functional insight into regulation of kinesin-1 by microtubule-associated protein MAP7. *Science* **375**, 326–331 (2022).
62. Hooy, R. M., Iwamoto, Y., Tudorica, D. A., Ren, X. & Hurley, J. H. Self-assembly and structure of a clathrin-independent AP-1:Arf1 tubular membrane coat. *Sci. Adv.* **8**, eadd3914 (2022).
63. Verbeke, E. J., Mallam, A. L., Drew, K., Marcotte, E. M. & Taylor, D. W. Classification of single particles from human cell extract reveals distinct structures. *Cell Rep.* **24**, 259–268.e3 (2018).
64. Kastritis, P. L. et al. Capturing protein communities by structural proteomics in a thermophilic eukaryote. *Mol. Syst. Biol.* **13**, 936 (2017).
65. Ho, C.-M. et al. Native structure of the RhopH complex, a key determinant of malaria parasite nutrient acquisition. *Proc. Natl Acad. Sci. USA* **118**, e2100514118 (2021).
66. Su, C.-C. et al. A 'build and retrieve' methodology to simultaneously solve cryo-EM structures of membrane proteins. *Nat. Methods* **18**, 69–75 (2021).
67. Danev, R. & Baumeister, W. Expanding the boundaries of cryo-EM with phase plates. *Curr. Opin. Struct. Biol.* **46**, 87–94 (2017).
68. Schwartz, O. et al. Laser phase plate for transmission electron microscopy. *Nat. Methods* **16**, 1016–1020 (2019).
    This study represents an exciting hardware development with impacts in the applicability and interpretability of both cryo-EM and cryo-ET by dramatically improving the contrast of the images and eliminating the requirement for large defocus.
69. Jijumon, A. S. et al. Lysate-based pipeline to characterize microtubule-associated proteins uncovers unique microtubule behaviours. *Nat. Cell Biol.* **24**, 253–267 (2022).
70. Yi, X., Verbeke, E. J., Chang, Y., Dickinson, D. J. & Taylor, D. W. Electron microscopy snapshots of single particles from single cells. *J. Biol. Chem.* **294**, 1602–1608 (2019).
71. Studer, D., Graber, W., Al-Amoudi, A. & Eggli, P. A new approach for cryofixation by high-pressure freezing. *J. Microsc.* **203**, 285–294 (2001).

72. Kuba, J. et al. Advanced cryo-tomography workflow developments—correlative microscopy, milling automation and cryo-lift-out. *J. Microsc.* **281**, 112–124 (2021).
73. Engel, L. et al. Lattice micropatterning for cryo-electron tomography studies of cell–cell contacts. *J. Struct. Biol.* **213**, 107791 (2021).
74. Toro-Nahuelpan, M. et al. Tailoring cryo-electron microscopy grids by photo-micropatterning for in-cell structural studies. *Nat. Methods* **17**, 50–54 (2020).
75. Gorelick, S. et al. PIE-scope, integrated cryo-correlative light and FIB/SEM microscopy. *eLife* **8**, e45919 (2019).
76. Boltje, D. B. et al. A cryogenic, coincident fluorescence, electron, and ion beam microscope. *eLife* **11**, e82891 (2022).
77. Smeets, M. et al. Correlative cryo-FIB milling using METEOR, an integrated fluorescent light microscope. *Microsc. Microanal.* **28**, 1310–1310 (2022).
78. Li, W. et al. Integrated multimodality microscope for accurate and efficient target-guided cryo-lamellae preparation. *Nat. Methods* **20**, 268–275 (2023).
79. Klumpe, S. et al. A modular platform for automated cryo-FIB workflows. *eLife* **10**, e70506 (2021).
80. Dutka, M. & Prokhodtseva, A. AutoTEM 5—fully automated TEM sample preparation for materials science. *Microsc. Microanal.* **25**, 554–555 (2019).
81. Eisenstein, F., Danev, R. & Pilhofer, M. Improved applicability and robustness of fast cryo-electron tomography data acquisition. *J. Struct. Biol.* **208**, 107–114 (2019).
82. Eisenstein, F. et al. Parallel cryo electron tomography on in situ lamellae. *Nat. Methods* **20**, 131–138 (2023).
83. Khavnekar, S. et al. Multishot tomography for high-resolution in situ subtomogram averaging. *J. Struct. Biol.* **215**, 107911 (2023).
84. Krull, A., Buchholz, T.-O. & Jug, F. Noise2Void—learning denoising from single noisy images. In *IEEE/CVF Conference on Computer Vision and Pattern Recognition (CVPR)* https://doi.org/10.1109/CVPR.2019.00223 (2019).
85. Lehtinen, J. et al. Noise2Noise: learning image restoration without clean data. In *Proc. 35th Intl Conf. Machine Learning*, PMLR 80, 2965–2974 (2018).
86. Liu, Y.-T. et al. Isotropic reconstruction for electron tomography with deep learning. *Nat. Commun.* **13**, 6482 (2022).
87. Böhm, J. et al. Toward detecting and identifying macromolecules in a cellular context: template matching applied to electron tomograms. *Proc. Natl Acad. Sci. USA* **97**, 14245–14250 (2000).
This study developed the computational method, tested in "phantom" cells, that allows localization of macromolecular complexes with known structures in cryo-ET data.
88. de Teresa-Trueba, I. et al. Convolutional networks for supervised mining of molecular patterns within cellular context. *Nat. Methods* **20**, 284–294 (2023).
89. Moebel, E. et al. Deep learning improves macromolecule identification in 3D cellular cryo-electron tomograms. *Nat. Methods* **18**, 1386–1394 (2021).
90. Rice, G. et al. TomoTwin: generalized 3D localization of macromolecules in cryo-electron tomograms with structural data mining. *Nat. Methods* **20**, 871–880 (2023).
91. Arnold, J. et al. Site-specific cryo-focused ion beam sample preparation guided by 3D correlative microscopy. *Biophys. J.* **110**, 860–869 (2016).
92. Ganeva, I. & Kukulski, W. Membrane architecture in the spotlight of correlative microscopy. *Trends Cell Biol.* **30**, 577–587 (2020).
93. Kukulski, W. et al. Correlated fluorescence and 3D electron microscopy with high sensitivity and spatial precision. *J. Cell Biol.* **192**, 111–119 (2011).
94. Sartori, A. et al. Correlative microscopy: bridging the gap between fluorescence light microscopy and cryo-electron tomography. *J. Struct. Biol.* **160**, 135–145 (2007).
95. Dahlberg, P. D. & Moerner, W. E. Cryogenic super-resolution fluorescence and electron microscopy correlated at the nanoscale. *Annu. Rev. Phys. Chem.* **72**, 253–278 (2021).
96. Dahlberg, P. D. et al. Cryogenic single-molecule fluorescence annotations for electron tomography reveal in situ organization of key proteins in *Caulobacter*. *Proc. Natl Acad. Sci. USA* **117**, 13937–13944 (2020).
97. Tuijtel, M. W., Koster, A. J., Jakobs, S., Faas, F. G. A. & Sharp, T. H. Correlative cryo super-resolution light and electron microscopy on mammalian cells using fluorescent proteins. *Sci. Rep.* **9**, 1369 (2019).
98. Wang, Q., Mercogliano, C. P. & Löwe, J. A ferritin-based label for cellular electron cryotomography. *Structure* **19**, 147–154 (2011).
99. Silvester, E. et al. DNA origami signposts for identifying proteins on cell membranes by electron cryotomography. *Cell* **184**, 1110–1121.e16 (2021).
100. Fung, H. K. H. et al. Genetically encoded multimeric tags for subcellular protein localization in cryo-EM. *Nat. Methods* **20**, 1900–1908 (2023).
101. Schorb, M., Haberbosch, I., Hagen, W. J. H., Schwab, Y. & Mastronarde, D. N. Software tools for automated transmission electron microscopy. *Nat. Methods* **16**, 471–477 (2019).
102. Lucas, B. A. & Grigorieff, N. Quantification of gallium cryo-FIB milling damage in biological lamellae. *Proc. Natl Acad. Sci. USA* **120**, e2301852120 (2023).
103. Berger, C. et al. Plasma FIB milling for the determination of structures in situ. *Nat. Commun.* **14**, 629 (2023).
104. Laughlin, T. G. et al. Architecture and self-assembly of the jumbo bacteriophage nuclear shell. *Nature* **608**, 429–435 (2022).
105. Lacey, S. E., Foster, H. E. & Pigino, G. The molecular structure of IFT-A and IFT-B in anterograde intraflagellar transport trains. *Nat. Struct. Mol. Biol.* **30**, 584–593 (2023).
106. Wozny, M. R. et al. In situ architecture of the ER–mitochondria encounter structure. *Nature* https://doi.org/10.1038/s41586-023-06050-3 (2023).
107. Baek, M. et al. Accurate prediction of protein structures and interactions using a three-track neural network. *Science* **373**, 871–876 (2021).
108. Jumper, J. et al. Highly accurate protein structure prediction with AlphaFold. *Nature* **596**, 583–589 (2021).
109. Graziadei, A. & Rappsilber, J. Leveraging crosslinking mass spectrometry in structural and cell biology. *Structure* **30**, 37–54 (2022).
110. O'Reilly, F. J. et al. In-cell architecture of an actively transcribing-translating expressome. *Science* **369**, 554–557 (2020).
This study combines cellular cryo-ET with in-cell crosslinking and whole-cell proteomics, and illustrates the power of integrative approaches to capture elusive and transient complexes.
111. Lucas, B. A. et al. Locating macromolecular assemblies in cells by 2D template matching with cisTEM. *eLife* **10**, e68946 (2021).
112. Rickgauer, J. P., Grigorieff, N. & Denk, W. Single-protein detection in crowded molecular environments in cryo-EM images. *eLife* **6**, e25648 (2017).
113. Lucas, B. A., Himes, B. A. & Grigorieff, N. Baited reconstruction with 2D template matching for high-resolution structure determination in vitro and in vivo without template bias. *eLife* **12**, RP90486 (2023).
114. Narayan, K. & Subramaniam, S. Focused ion beams in biology. *Nat. Methods* **12**, 1021–1031 (2015).
115. Xu, C. S. et al. An open-access volume electron microscopy atlas of whole cells and tissues. *Nature* **599**, 147–151 (2021).
116. Smith, D. & Starborg, T. Serial block face scanning electron microscopy in cell biology: applications and technology. *Tissue Cell* **57**, 111–122 (2019).
117. Harkiolaki, M. et al. Cryo-soft X-ray tomography: using soft X-rays to explore the ultrastructure of whole cells. *Emerg. Top. Life Sci.* **2**, 81–92 (2018).
118. Mahamid, J. et al. Visualizing the molecular sociology at the HeLa cell nuclear periphery. *Science* **351**, 969–972 (2016).
119. Kasinath, V. et al. JARID2 and AEBP2 regulate PRC2 in the presence of H2AK119ub1 and other histone modifications. *Science* **371**, eabc3393 (2021).
120. Mosalaganti, S. et al. AI-based structure prediction empowers integrative structural analysis of human nuclear pores. *Science* **376**, eabm9506 (2022).
This study capitalizes on AlphaFold2 and cryo-ET data for structural modelling of the human nuclear pore complex with unprecedented precision and completeness.
121. Gemmer, M. et al. Visualization of translation and protein biogenesis at the ER membrane. *Nature* **614**, 160–167 (2023).
122. Hoffmann, P. C. et al. Tricalbins contribute to cellular lipid flux and form curved ER–PM contacts that are bridged by rod-shaped structures. *Dev. Cell* **51**, 488–502.e8 (2019).
123. Lucas, B. A., Zhang, K., Loerch, S. & Grigorieff, N. In situ single particle classification reveals distinct 60S maturation intermediates in cells. *eLife* **11**, e79272 (2022).
124. De Rosier, D. J. & Klug, A. Reconstruction of three dimensional structures from electron micrographs. *Nature* **217**, 130–134 (1968).
125. Dubochet, J. & McDowall, A. W. Vitrification of pure water for electron microscopy. *J. Microsc.* **124**, RP3–RP4 (1981).
126. Frank, J. Averaging of low exposure electron micrographs of non-periodic objects. *Ultramicroscopy* **1**, 159–162 (1975).
127. Hart, R. G. Electron microscopy of unstained biological material: the polytropic montage. *Science* **159**, 1464–1467 (1968).
128. Cheng, Y., Grigorieff, N., Penczek, P. A. & Walz, T. A primer to single-particle cryo-electron microscopy. *Cell* **161**, 438–449 (2015).
129. Chen, Z. et al. In situ cryo-electron tomography reveals the asymmetric architecture of mammalian sperm axonemes. *Nat. Struct. Mol. Biol.* **30**, 360–369 (2023).
130. Hoffmann, P. C. et al. Structures of the eukaryotic ribosome and its translational states in situ. *Nat. Commun.* **13**, 7435 (2022).
131. Wan, W. & Briggs, J. A. G. Cryo-electron tomography and subtomogram averaging. *Methods Enzymol.* **579**, 329–367 (2016).
132. Wang, Z. et al. The molecular basis for sarcomere organization in vertebrate skeletal muscle. *Cell* **184**, 2135–2150.e13 (2021).
133. Pyle, E. & Zanetti, G. Current data processing strategies for cryo-electron tomography and subtomogram averaging. *Biochem. J.* **478**, 1827–1845 (2021).
134. wwPDB Consortium. Protein Data Bank: the single global archive for 3D macromolecular structure data. *Nucleic Acids Res.* **47**, D520–D528 (2018).
135. Lawson, C. L. et al. EMDataBank unified data resource for 3DEM. *Nucleic Acids Res.* **44**, D396–D403 (2016).
136. Iudin, A. et al. EMPIAR: the Electron Microscopy Public Image Archive. *Nucleic Acids Res.* **51**, D1503–D1511 (2023).

Acknowledgements We are grateful to our group members and many colleagues for fruitful discussions. We thank those who provided figures for reproduction in this Review, and we apologize to those whose outstanding work we have not been able to cite due to the limited number of references. E.N. acknowledges support from the US National Institutes of Health (R35GM127018), the European Research Council (ERC-2022-SYG 101071583), and is a Howard Hughes Medical Institute Investigator. J.M. acknowledges valuable assistance from J. Dobbs, support from the EMBL, a European Research Council starting grant (3DCellPhase 760067) and a Chan-Zuckerberg Initiative grant for Visual Proteomics.

Author contributions E.N. and J.M. contributed to the conception, writing and editing of the manuscript.

Competing interests The authors declare no competing interests.

Additional information

Correspondence and requests for materials should be addressed to Eva Nogales or Julia Mahamid.

Peer review information *Nature* thanks A. Radu Aricescu and the other, anonymous, reviewer(s) for their contribution to the peer review of this work.